Chinese Chemical Letters 36 (2025) 109678

Contents lists available at ScienceDirect

Chinese Chemical Letters

journal homepage: www.elsevier.com/locate/cclet

N-Benzyl arylamide derivatives as novel and potent tubulin polymerization inhibitors against gastric cancers: Design, structure–activity relationships and biological evaluations

Jian Song[a,1], Shenghui Wang[a,1], Qiuge Liu[a], Xiao Wang[a], Shuo Yuan[d], Hongmin Liu[b,*], Saiyang Zhang[a,c,*]

[a] *School of Basic Medical Sciences, Zhengzhou University, Zhengzhou 450001, China*
[b] *School of Pharmaceutical Sciences, Institute of Drug Discovery & Development, Key Laboratory of Advanced Drug Preparation Technologies (Ministry of Education), Zhengzhou University, Zhengzhou 450001, China*
[c] *State Key Laboratory of Esophageal Cancer Prevention & Treatment, Zhengzhou 450001, China*
[d] *Children's Hospital Affiliated to Zhengzhou University, Henan Children's Hospital, Zhengzhou Children's Hospital, Zhengzhou 450018, China*

ARTICLE INFO

Article history:
Received 2 January 2024
Revised 20 February 2024
Accepted 22 February 2024
Available online 28 February 2024

Keywords:
Tubulin
Colchicine binding site
CA-4
N-Benzyl arylamide
Antiproliferative activities

ABSTRACT

In this work, we employed a ring-opening strategy to develop a series of novel *N*-benzyl arylamide derivatives as tubulin polymerization inhibitors. Notably, **13n** (**MY-1388**) exhibited remarkable antiproliferative potency on fifteen human cancer cell lines, with half maximal inhibitory concentration (IC_{50}) values ranging from 8 nmol/L to 48 nmol/L. Furthermore, **13n** effectively suppressed tubulin polymerization by targeting the colchicine-binding site ($IC_{50} = 0.62$ μmol/L). **13n** also exhibited significant inhibition of cell colony formation, as well as displayed potent effects on inducing G2/M phase cell cycle arrest and promoting apoptosis. Importantly, **13n** exhibited enhanced and adequate liver microsomal stability in human and rat liver microsomes, and also exhibited a moderate half-life ($T_{1/2} = 0.938$ h) *in vivo*. Meanwhile, **13n** demonstrated effective antitumor effects *in vivo* in suppressing tumor growth in the MGC-803 xenograft model (tumor growth inhibition (TGI) value was 76.4% at the dosage of 30 mg kg^{-1} day^{-1}) with a good safety profile. Collectively, these results revealed that **13n** represents a promising tubulin polymerization inhibitor that deserves further investigation for its efficacy in treating gastric cancers.

Microtubules, as the crucial component of the tumor cell cytoskeleton, play pivotal roles in essential biological functions such as mitosis, cell signaling, and intracellular transport [1,2]. Consequently, microtubules have emerged as significant and highly efficacious targets for cancer treatment [3,4]. By interfering with microtubule dynamics, microtubule-targeting agents (MTAs) could effectively induce cycle arrest and apoptosis in tumor cells, thus exhibiting potent anti-tumor effects. Some of MTAs, such as paclitaxel and vinblastine along with their analogues, have gained U.S. Food and Drug Administration (FDA) approval for frontline cancer treatment [5]. Nevertheless, these drugs still encounter certain limitations in clinical application due to concerns regarding drug toxicity and resistance [4,6].

Currently, seven binding sites on microtubules have been identified, including the paclitaxel site, vinca site, laulimalide site, pironetin site, maytansine site, colchicine site and the seventh site [7–9]. Among them, the MTAs targeting the colchicine binding site (colchicine binding site inhibitors or CBSIs) have garnered significant attention due to their favorable attributes compared to other MTAs, such as simplistic structures, enhanced water solubility, wide therapeutic index, and diminished multi-drug resistance [10,11]. To date, some CBSIs, such as, OXI4503 [12], AVE8062 [13], BNC-105P [14] and ABT-751 [15], have been or are being investigated in clinical trials for cancer therapy (Fig. 1A).

The natural product combretastatin A-4 (CA-4, **1**), derived from the South African bushwillow tree *Combretum caffrum*, demonstrates potent inhibitory activity against a variety of tumor cells [16]. CA-4 exerts its effects by targeting the colchicine binding site, leading to disrupt cell mitosis and induce cell apoptosis [17]. Despite the significant *in vitro* anti-tumor activity of CA-4, its lower bioavailability and less effective activity *in vivo*, further limited its clinical applications [18]. As a result, numerous research groups have conducted extensive structural modifications on CA-4 [17,19-21], with some derivatives such as OXI4503 and AVE8062, success-

* Corresponding authors.
E-mail addresses: liuhm@zzu.edu.cn (H. Liu), saiyangz@zzu.edu.cn (S. Zhang).
[1] These authors contributed equally to this work.

https://doi.org/10.1016/j.cclet.2024.109678
1001-8417/

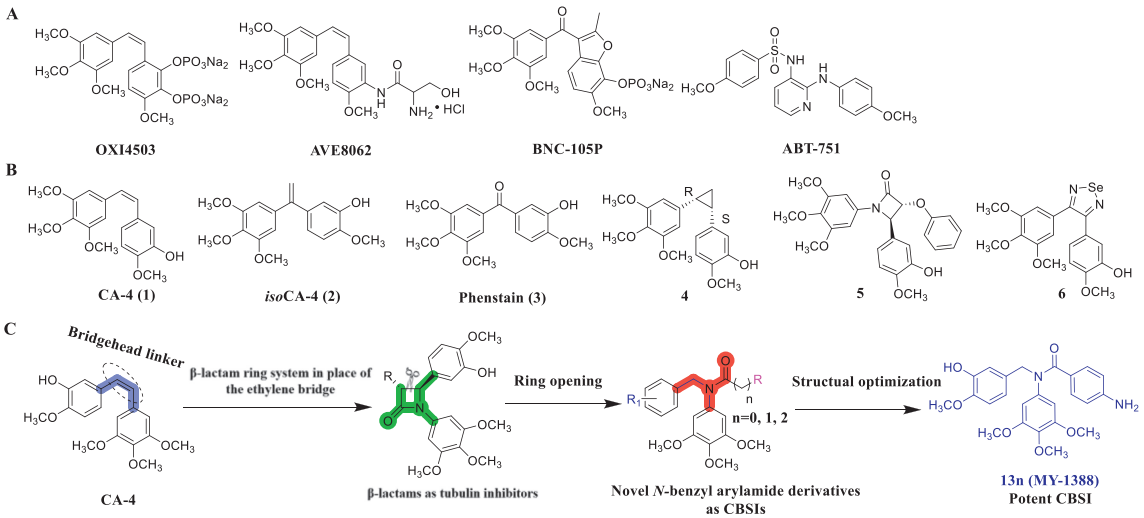

Fig. 1. (A) Representative CBSIs that have been approved for clinical trials. (B) CA-4 and representative CA-4 analogues as CBSIs. (C) Design of *N*-benzyl arylamide derivatives as CBSIs in this work.

fully entering clinical trials. In the researches on structural modifications of CA-4, the *cis*-ethylene bridge in the structure of CA-4 was usually modified, such as replacing it with a longer or shorter connecting chain or directly modifying the double bond [22–26]. For example, compounds *iso*CA-4 (**2**) and phenstain (**3**) were also exhibited excellent antitumor properties [27]. In addition, by replacing the *cis*-ethylene bridge with a rigid cyclic system consisting of three to six-membered rings, flipping could be prevented, thereby increasing stability and maintaining biological activity [28–30]. This approach also enables the synthesis of compounds exhibiting excellent antitumor activity, such as cyclopropyl analog **4** [29], β-lactam **5** [31] and 1,2,5-selenadiazol **6** (Fig. 1B) [30].

Many groups have incorporated the *cis*-double bond of CA-4 into a rigid β-lactam ring to design and synthesize β-lactam-based CBSIs [32–36], which exhibit excellent inhibitory activity against tubulin polymerization with potent anti-tumor activities. However, β-lactam compounds, especially β-lactam antibiotics, with chiral centers, may undergo hydrolysis or molecular rearrangement, leading to loss of efficacy and further limiting clinical applications [37,38]. In addition, as a commonly found structural fragment in FDA-approved small molecule compounds, the amide scaffold is frequently in the design of anticancer agents [39–41]. Hence, we attempted to obtain the amide scaffold unit by opening up the β-lactam ring to circumvent potential disadvantages associated with β-lactams (Fig. 1C). By employing the ring-opening approach, we here try to transform the β-lactam scaffold-based inhibitors derived from CA-4 into an *N*-benzyl arylamide scaffold, which was then used to derive novel *N*-benzyl arylamide derivatives. Meanwhile, in the design of *N*-benzyl arylamide derivatives, the 3,4,5-trimethoxyphenyl moiety was retained, which is considered as an essential active moiety to act on colchicine binding site [20]. We found that novel *N*-benzyl arylamide derivative **13n** (also known as **MY-1388**), whose mechanism is the inhibition of tubulin polymerization by targeting the colchicine binding site, demonstrated excellent *in vivo* and *in vitro* activities.

The synthetic procedures of compounds **13a–ac**, **14a–k** and **16a–g** were illustrated in Scheme S1 (Supporting information). Under standard aldimine condensation reaction conditions, substituted aromatic aldehydes **7a–i** were reacted with 3,4,5-trimethoxyaniline (**8**) to afford schiff bases **9a–i**, which were reduced by sodium borohydride to generate the intermediates **10a–i**. Substitution reactions of compound **10a** with commercially-available acyl chlorides (**11a–z** and **12a–k)** gave the final products **13a–m**, **13o–y**, **13aa–ab** and **14a–k**. The amino compounds **13m**, **13y** and **13ac** were prepared by the reduction reactions of nitros **13n**, **13z** and **13ab**. Under the substitution reaction conditions, compounds **10b–i** reacted with 4-nitrobenzoyl chloride (**12m**) to get intermediates **15a–g**. Subsequently, intermediates **15a–g** were reduced by Fe to obtain the final products **16a–g**.

Given these compounds were designed as anticancer agents, the *in vitro* antiproliferative activities of **13a–ac**, **14a–k** and **16a–g** were first explored *via* using the MTT assay MGC-803 (human gastric cancer cell line), KYSE450 (human esophageal cancer cell line), and HCT-116 (human colorectal cancer cell line) after a 48-h incubation period with two well-known CBSIs, colchicine and CA-4, as positive control drugs.

As shown in Table S1 (Supporting information), *N*-benzyl arylamides **13a** to **13z** exhibited excellent antiproliferative activities against these three cancer cells *in vitro*, with half maximal inhibitory concentration (IC_{50}) values all below 0.5 μmol/L. Among them, **13a**, **13b**, **13c**, **13g**, **13h**, **13i**, **13n** (also known as **MY-1388**) and **13w** showed the best activity within the range of IC_{50} values from 0.09 μmol/L to 0.047 μmol/L. Particularly, **13n** (**MY-1388**) with an amino-substituted group on right-side phenyl ring demonstrated the strongest activity, displaying excellent IC_{50} values of 0.009 μmol/L for MGC-803 cells, 0.018 μmol/L for HCT-116 cells and 0.014 μmol/L for KYSE450 cells respectively, surpassing colchicine. Importantly, it exhibited comparable CA-4-like activity ($IC_{50} = 0.008$ μmol/L) in inhibiting MGC-803 cells.

Further elucidating the structure-activity relationship, it was observed that substituents on right-side phenyl ring exert an influence on the *in vitro* antiproliferative activities. **13a** demonstrated notable antiproliferative activity (MGC-803: $IC_{50} = 0.027$ μmol/L) when devoid of substituents on the right-side phenyl ring. When electron-donating groups such as methyl, methoxy, and amino were introduced as *para*-substituents on the right-side phenyl ring, **13b**, **13c** and **13n** (**MY-1388**) exhibited enhanced antiproliferative potency against MGC-803 cells. Conversely, when these substituents were positioned at the meta-position of right-side phenyl ring (**13e** and **13f**), their activity decreased compared to **13a**, **13b** and **13c**. In comparison to **13a**, compounds containing electron-donating groups like *tert*-butyl and dimethylamino as *para*-substituents on the right-side phenyl ring (**13d** and **13l**) displayed reduced activities against MGC-803 cells. Compared to **13a**, the activity of the compound weakens as the electron-withdrawing effect strengthens when the *para*-substituents the

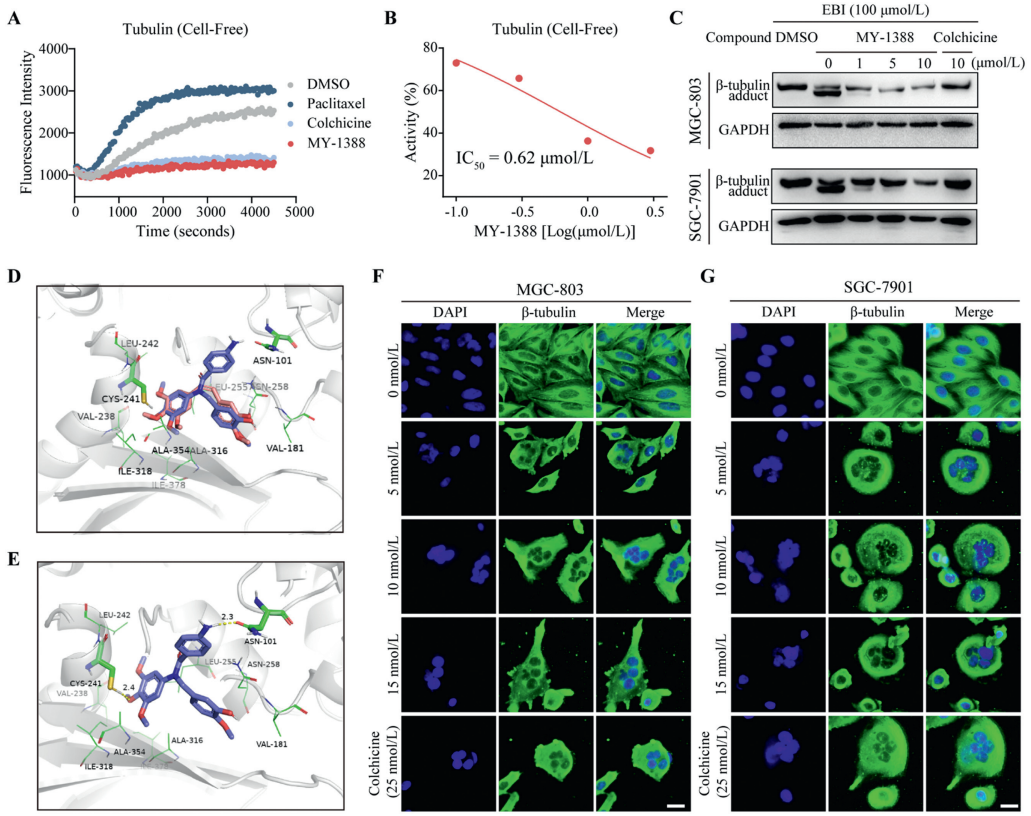

Fig. 2. Compound **MY-1388** bound to colchicine binding site to inhibit tubulin polymerization. (A) Cell-free tubulin polymerization detection, the fluorescence intensity indicates the level of tubulin polymerization. (B) The activity percentage of tubulin treated with compound **MY-1388**. (C) *N*,*N*′-Ethylene-bis(iodoacetamide) (EBI) competition assay. Immunoblotting analysis for β-tubulin adduct protein and glyceraldehyde-3-phosphate dehydrogenase (GAPDH) protein from MGC-801 and SGC-7901 cells. (D, E) Molecular docking models between compound **MY-1388** with tubulin (PDB: 5LYJ). The binding mode comparison between compound **MY-1388** with CA-4 (D). The proposed binding mode of compound **MY-1388** in the colchicine binding site of β-tubulin (E). The hydrogen bonds were shown in yellow dotted lines. (F, G) Effects of compound **MY-1388** on microtubule networks. Microtubules were visualized with an anti-β-tubulin antibody (green), and the cell nucleus was visualized with 4′,6-diamidino-2-phenylindole (DAPI, blue). Scale bar: 25 μm.

right-side phenyl ring are F, Cl, Br, CF_3, CN or NO_2. Among them, **13g**, **13h** and **13i** demonstrated superior activities compared to compound **13a**. Similarly, the electron-withdrawing groups on the right-side phenyl ring as *meta*-substituents showed weaker activity than those as *para*-substituents (**13g** *vs.* **13p**; **13h** *vs.* **13q**; **13i** *vs.* **13r**). To further investigate the structure-activity relationship, **13s**–**ac** were designed and synthesized to explore the impact of alkyl chain length (n) on activities (Table S1), compared to **13a**–**r**, the activity of the decreases **13s**–**ac** with the same substituent as the length (n) of the alkyl chain increases (**13a** *vs.* **13s** *vs.* **13aa**, **13b** *vs.* **13t**, **13c** *vs.* **13u**, **13g** *vs.* **13v**, **13h** *vs.* **13w**, **13i** *vs.* **13x**, **13m** *vs.* **13y** *vs.* **13ab**, **13n** *vs.* **13z** *vs.* **13ac**).

Subsequently, the right-side phenyl ring was substituted with heterocyclic groups such as thiophene, furan and pyridine (**14a**–**k**, Table S2 in Supporting information). Concurrently, the impact of alkyl chain length (n) on compound activity was also investigated. Most of the **14a**–**k** exhibited potent antiproliferative activities against these three cancer cells, with IC_{50} values ranging from 0.011 μmol/L to 0.37 μmol/L. In addition, **14a**, **14d** and **14e** featuring unsubstituted thiophene, furan and pyridine moieties demonstrated exceptional activity, surpassing **14b**, **14c**, **14f** and **14g** containing substituted thiophene and pyridine moieties. Among them, **14a** and **14d** exhibited slightly lower activity than **13n** (**MY-1388**), with IC_{50} values ranging from 0.011 μmol/L to 0.020 μmol/L. Similarly, an increase in alkyl chain length (n) results in a decrease in activities, as evidenced by the comparison of **14a** *vs.* **14h** *vs.* **14j**, **14d** *vs.* **14k**, **14e** *vs.* **14i**.

Next, we continued to change the substituents on left-side phenyl ring to synthesize **16a**–**g** (Table S3 in Supporting information). However, the results revealed that modifications of the left-side phenyl ring led to a significant reduction in antiproliferative activities. Compared to **16g**, the incorporation of a hydroxy group (**MY-1388**) at the *meta*-position of the left-side phenyl ring could significantly enhance the antiproliferative activities. The introduction of electron-donating group (methoxy) or electron-withdrawing groups (F, Cl, Br) on the *meta*-position significantly diminished the antiproliferative activities, compared to **16g**. Compared with **13n** (**MY-1388**), **16f**, which retains only the *meta*-hydroxy substituent, exhibited a significantly reduced antiproliferative activity. On the other hand, **16g**, which only retains a methoxy substituent at the *para*-position, maintained its antiproliferative activity at nanomolar levels. These results indicated that the presence of a *para*-methoxy group on the left-side phenyl ring is crucial for maintaining antiproliferative activity, and the *meta*-hydroxy substitution significantly enhanced its potency.

Considering that **MY-1388** exhibited excellent proliferative inhibition activity against MGC-803, HCT-116 and KYSE450 cells, its antiproliferative potency on other 15 cancer cells, gastric normal cells GES-1, and normal vascular endothelial cells HUVEC were also further evaluated using MTT assay (Table S4 in Supporting information). **MY-1388** also exhibited a broad spectrum of antiproliferative activity against other 12 cancer cells with IC_{50} values ranging from 0.008 μmol/L to 0.048 μmol/L with high selective inhibitory activities over normal cells GES-1 (IC_{50} = 0.76 μmol/L) and HUVEC

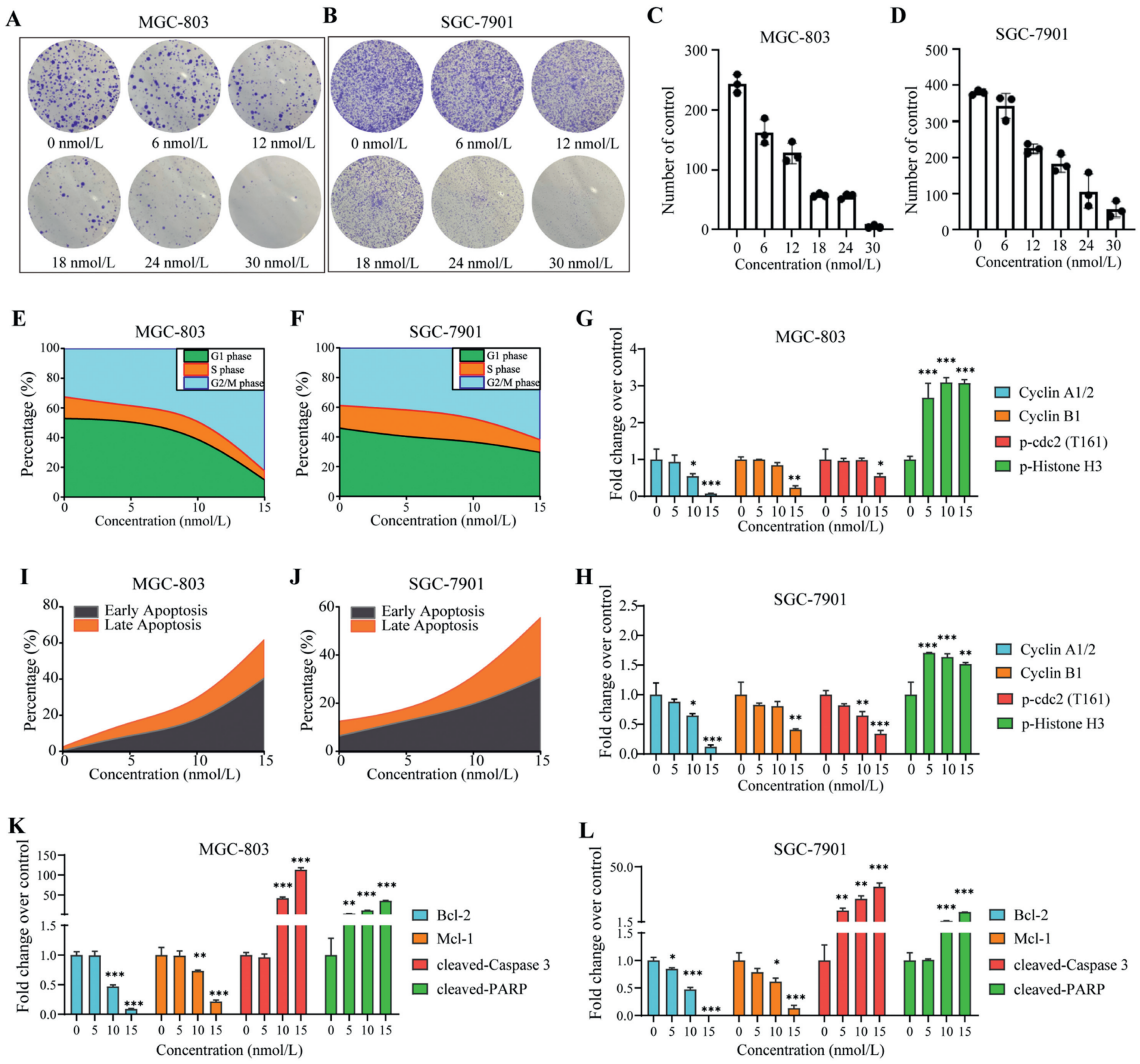

Fig. 3. Effects of compound **MY-1388** on cell colony formatting ability, cell cycle and apoptosis. Cells were treated for 48 h. (A–D) Images of formatted cell colonies. (E, F) Cell cycle distribution of treated cells detected by flow cytometry. (G, H) Levels of cell cycle related proteins. (I, J) Cell apoptosis ratio of treated cells detected by flow cytometry. (K, L) Level of cell apoptosis related proteins. Quantitative data were represented as the mean ± standard deviation (SD) ($n = 3$). $^{*}P < 0.05$, $^{**}P < 0.01$, $^{***}P < 0.001$ *vs.* the vehicle control.

($IC_{50} = 48.47$ μmol/L). Next, we also conducted further investigations to evaluate the potential of **MY-1388** overcome drug resistance. To accomplish this, three resistant cancer cell lines were selected: paclitaxel-resistant A549/Taxol cells, as well as multidrug-resistant MCF-7/ADR and SGC-7901/ADR cells. The results presented in Table S5 (Supporting information) demonstrate that **MY-1388** exhibited more potent antiproliferative activities compared to those of paclitaxel ($IC_{50} = 0.045$ *vs.* 0.23 μmol/L for A549/Taxol; 0.0227 *vs.* 5.23 μmol/L for MCF-7/ADR; 0.0188 *vs.* 6.27 μmol/L for SGC-7901/ADR).

These compounds were designed as a specific tubulin polymerization inhibitor by targeting the colchicine binding site of β-tubulin. Therefore, the effects of **MY-1388** on tubulin polymerization were further evaluated. As shown in Figs. 2A and B, **MY-1388** could concentration-dependently inhibit tubulin polymerization under cell-free condition with an IC_{50} value of 0.62 μmol/L, which was better than that of colchicine ($IC_{50} = 6.7$ μmol/L) [42] and CA-4 ($IC_{50} = 1.98$ μmol/L) [43], and could directly interacted with the colchicine binding site of β-tubulin (Fig. 2C). To predict the binding modes of **MY-1388** with tubulin, molecular docking studies were further explored (PDB: 5LYJ) by MOE.2019.01 software. The docking results indicated that **MY-1388** could well bind into the colchicine binding site of β-tubulin (Fig. 2E), and it shared similar binding modes with CA-4 (Fig. 2D). The 4-methoxy group could form a hydrogen bond with Cys241 at a distance of 2.4 Å. At the same time, the 3-hydroxy-4-methoxyphenyl group could engage in extensive hydrophobic interactions with surrounding amino acid residues, including Leu242, Val238, Ala354 and Ile318. Compared CA-4, the 4-aminophenyl group formed an additional hydrogen bond with Asn101's backbone at a distance of 2.3 Å. The binding between **MY-1388** and colchicine binding site of β-tubulin is maintained through hydrogen bonding and hydrophobic interactions, resulting in its potent tubulin polymerization inhibitory activity. In addition, in **MY-1388** treated MGC-803 and SGC-7901 cells, multiple nuclei obtained from cell replication could not be drawn to complete mitosis, and the phenomenon of multiple nuclei appeared (Figs. 2F and G), which was similar to colchicine, indicating that **MY-1388** exerted a potent impact on the tubulin assembly and disrupting microtubule networks.

Inhibition of tubulin polymerization could result in mitotic arrest of cancer cells, thus inhibiting cell colony formatting ability, and inducing cell cycle arrest and cell apoptosis. Therefore, the effects of **MY-1388** on cell colony formatting ability, cell cycle arrest and apoptosis were further explored. After treatment with **MY-**

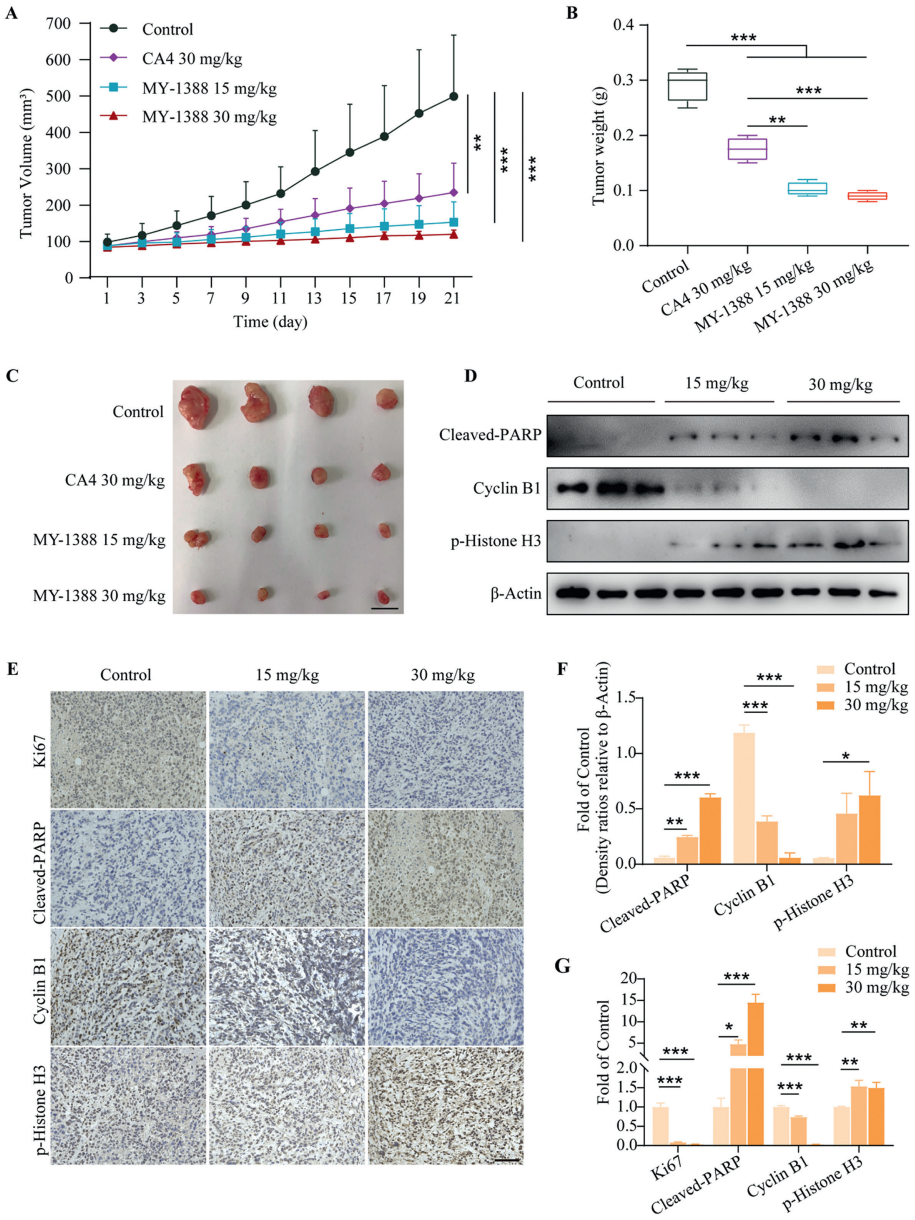

Fig. 4. Antitumor activity of compound **MY-1388** *in vivo*. (A) Tumor volume during the treatment. (B) Tumor weight of each group. (C) Images of tumor tissues. (D, F) Apoptosis and proliferation-related proteins levels detected by Western blot assay. Scale bar: 10 mm. (E, G) Protein levels detected by immunohistochemistry. Scale bar: 500 μm. Quantitative data were represented as the mean ± SD ($n = 3$). $^{*}P < 0.05$, $^{**}P < 0.01$, $^{***}P < 0.001$ *vs.* the vehicle control.

1388, cell colony formatting ability was concentration-dependently inhibited (Figs. 3A–D), and the morphological changes in MGC-803 and SGC-7901 cells were observed (Figs. S1A–C in Supporting information). In addition, **MY-1388** also displayed potent effects on inducing G2/M phase cell cycle arrest (Figs. 3E–H and Figs. S2A–D in Supporting information) and promoting apoptosis (Figs. 3I–L, and Figs. S2E–H in Supporting information) by modulating the expression levels of proteins involved in cell cycle and apoptosis.

In order to facilitate the development of candidate drugs, it is imperative to achieve a harmonious equilibrium between biological activity and physicochemical properties. **MY-1388** showed acceptable druglike properties according to the Lipinski's rule of five (Table S6 in Supporting information). In addition, **MY-1388** also exhibited good liver microsomal stability in human ($T_{1/2} = 37.5$ min) and rat liver ($T_{1/2} = 133$ min) microsomes (Table S7 in Supporting information). After 60 min incubations, while 32.0% and 73.9% of **MY-1388** still remained in human and rat liver microsomes, respectively. However, according to previous research, only 26.4% of CA-4 remained in rat liver microsomes [44]. Given **MY-1388** exhibited improved stability compared to CA-4 in the human liver microsome. A pharmacokinetic study *in vivo* was further performed for **MY-1388** in rats ($n = 3$) after intravenous injection (10 mg/kg). The results of Table S8 (Supporting information) indicated **MY-1388** was absorbed quickly ($T_{max} = 0.0833$ h) and exhibited a moderate half-life ($T_{1/2} = 0.938$ h).

In order to investigate the *in vivo* inhibitory effects of **MY-1388** on gastric cancer cells, a xenograft model bearing MGC-803 cells was established. CA-4 was used as a positive control and the **MY-1388** was administered daily by intraperitoneal injection. Animal welfare and experimental procedures have been reviewed and approved by the Animal Ethics Committee of Zhengzhou University, Zhengzhou, China. As shown in Fig. 4, compared to the negative control group, the CA-4 group (30 mg kg^{-1} day^{-1}), **MY-1388** group (15 mg kg^{-1} day^{-1}), and **MY-1388** group (30 mg kg^{-1} day^{-1}) ex-

hibited significantly reduced tumor volume and weight (Figs. 4A–C), and also exhibited a good safety profile (Fig. S3 in Supporting information). The tumor growth inhibition rates for the CA-4 group (30 mg kg^{-1} day^{-1}), **MY-1388** group (10 mg kg^{-1} day^{-1}), and **MY-1388** group (30 mg kg^{-1} day^{-1}) were 53.2%, 69.7%, and 76.4%, respectively, indicating that **MY-1388** demonstrated remarkable *in vivo* anti-tumor effects surpassing those of CA-4. In addition, the protein changes in tumor tissues were the same as *in vitro*, and **MY-1388** led to up-regulation of cleaved-poly ADP-ribose polymerase (cleaved-PARP), p-Histone H3, and down-regulation of Ki67, cyclin B1 (Figs. 4D–G).

In summary, we designed and synthesized a series of novel *N*-benzylaryl amide derivatives as CSBIs with potential anticancer by ring-opening strategy. Among them, **13n** (**MY-1388**) exhibited excellent antiproliferative potency on fifteen human cancer cell lines with IC_{50} values ranging from 8 nmol/L to 48 nmol/L. Further studies confirmed that **13n** (**MY-1388**) could target the colchicine-binding site of β-tubulin, potently inhibited tubulin polymerization ($IC_{50} = 0.62$ μmol/L), significantly inhibited cell colony formation, and effectively induced G2/M phase cell cycle and cell apoptosis. Additionally, **13n** (**MY-1388**) shows enhanced and adequate liver microsomal stability in human ($T_{1/2} = 37.5$ min) and rat liver ($T_{1/2} = 133$ min) microsomes. Importantly, **13n** (**MY-1388**) demonstrated potent antitumor effects (TGI rate was 76.4% at a dosage of 30 mg/kg) with a favorable safety profile in an MGC-803 xenograft model, surpassing the antitumor efficacy of CA-4 (30 mg kg^{-1} day^{-1}). The aforementioned results demonstrate that **13n** (**MY-1388**) exhibits significant potential as a tubulin polymerization inhibitor, warranting further exploration for its development in cancer therapy.

Declaration of competing interest

The authors declare that they have no known competing financial interests or personal relationships that could have appeared to influence the work reported in this paper.

Acknowledgments

This work was supported by the National Natural Science Foundation of China (Nos. 82273782 and U2004123) and Training Program for Young Key Teachers of Colleges and Universities in Henan Province (No. 2023GGJS008).

Supplementary materials

Supplementary material associated with this article can be found, in the online version, at doi:10.1016/j.cclet.2024.109678.

References

[1] G.M. Alushin, G.C. Lander, E.H. Kellogg, et al., Cell 157 (2014) 1117–1129.
[2] C. Dumontet, M.A. Jordan, Nat. Rev. Drug Discov. 9 (2010) 790–803.
[3] A.C. Henriques, D. Ribeiro, J. Pedrosa, et al., Cancer Lett. 440-441 (2019) 64–81.
[4] M. Kavallaris, Nat. Rev. Cancer 10 (2010) 194–204.
[5] L. Wordeman, J.J. Vicente, Cancers 13 (2021) 194–204.
[6] M.A. Kamal, M.H. Al-Zahrani, S.H. Khan, et al., Curr. Drug Metab. 21 (2020) 178–185.
[7] M.O. Steinmetz, A.E. Prota, Trends. Cell Biol. 28 (2018) 776–792.
[8] Y.F. Zhang, J. Huang, W.X. Zhang, et al., Bioorg. Chem. 139 (2023) 106684.
[9] J. Yang, Y. Yu, Y. Li, et al., Sci. Adv. 7 (2021) eabg4168.
[10] E.C. McLoughlin, N.M. O'Boyle, Pharmaceuticals 13 (2020) 8.
[11] M. Hawash, Biomolecules 12 (2022) 1843.
[12] J. Cummings, M. Zweifel, N. Smith, et al., Br. J. Cancer 106 (2012) 1766–1771.
[13] C. Sessa, P. Lorusso, A. Tolcher, et al., Clin. Cancer Res. 19 (2013) 4832–4842.
[14] S. Pal, A. Azad, S. Bhatia, et al., Clin. Cancer Res. 21 (2015) 3420–3427.
[15] C.M. Rudin, A. Mauer, M. Smakal, et al., J. Clin. Oncol. 29 (2011) 1075–1082.
[16] G.M. Tozer, C. Kanthou, C.S. Parkins, S.A. Hill, Int. J. Exp. Pathol. 83 (2002) 21–38.
[17] M.J. Pérez-Pérez, E.M. Priego, O. Bueno, et al., J. Med. Chem. 59 (2016) 8685–8711.
[18] G.C. Tron, T. Pirali, G. Sorba, et al., J. Med. Chem. 49 (2006) 3033–3044.
[19] S. Paidakula, S. Nerella, S. Kankala, R.K. Kankala, Curr. Med. Chem. 29 (2022) 3748–3773.
[20] L. Li, S. Jiang, X. Li, et al., Eur. J. Med. Chem. 151 (2018) 482–494.
[21] L.M. Nainwal, M.M. Alam, M. Shaquiquzzaman, A. Marella, A. Kamal, Expert. Opin. Ther. Pat. 29 (2019) 703–731.
[22] W. Li, Y. Yin, H. Yao, et al., Eur. J. Med. Chem. 157 (2018) 1068–1080.
[23] X.Y. Yuan, C.H. Song, X.J. Liu, et al., Eur. J. Med. Chem. 252 (2023) 115281.
[24] J. Song, S.H. Wang, C.H. Song, et al., Eur. J. Med. Chem. 240 (2022) 114583.
[25] X.Y. Shi, H. Jiao, J.K. Zhang, et al., J. Enzyme. Inhib. Med. Chem. 38 (2023) 2237701.
[26] J.H. Jiang, C.H. Zheng, C.Q. Wang, et al., Chin. Chem. Lett. 26 (2015) 607–609.
[27] S. Messaoudi, B. Tréguier, A. Hamze, et al., J. Med. Chem. 52 (2009) 4538–4542.
[28] S. Theeramunkong, A. Caldarelli, A. Massarotti, et al., J. Med. Chem. 54 (2011) 4977–4986.
[29] N. Ty, R. Pontikis, G.G. Chabot, et al., Bioorg. Med. Chem. 21 (2013) 1357–1366.
[30] Q. Guan, F. Yang, D. Guo, et al., Eur. J. Med. Chem. 87 (2014) 1–9.
[31] T.F. Greene, S. Wang, L.M. Greene, et al., J. Med. Chem. 59 (2016) 90–113.
[32] R. Ramajayam, Eur. J. Med. Chem. 162 (2019) 1–17.
[33] P. Zhou, Y. Liu, L. Zhou, et al., J. Med. Chem. 59 (2016) 10329–10334.
[34] N.M. O'Boyle, M. Carr, L.M. Greene, et al., J. Med. Chem. 53 (2010) 8569–8584.
[35] A.M. Malebari, D. Fayne, S.M. Nathwani, et al., Eur. J. Med. Chem. 189 (2020) 112050.
[36] E.C. McLoughlin, B. Twamley, J.E. O'Brien, et al., Bioorg. Chem. 141 (2023) 106877.
[37] L.M. Lima, B. Silva, G. Barbosa, E.J. Barreiro, Eur. J. Med. Chem. 208 (2020) 112829.
[38] W. Xu, Z. Ma, G. Dhanda, J. Haldar, H. Xie, Chin. Chem. Lett. 34 (2023) 107847.
[39] S. Yuan, D.S. Wang, H. Liu, et al., Eur. J. Med. Chem. 245 (2023) 114898.
[40] S. Yuan, D.D. Shen, R. Jia, et al., Med. Res. Rev. 43 (2023) 2352–2391.
[41] J. He, Z. Li, G. Dhawan, et al., Chin. Chem. Lett. 34 (2023) 107578.
[42] J. Song, Y.F. Guan, W.B. Liu, et al., Eur. J. Med. Chem. 238 (2022) 114467.
[43] H. Zhu, Y. Tan, C. He, Y. Liu, et al., J. Med. Chem. 65 (2022) 11187–11213.
[44] Y. Pang, B. An, L. Lou, et al., J. Med. Chem. 60 (2017) 7300–7314.